ChemComm

High yield synthesis and surface chemistry exchange of small gold hexagonal nanoprisms

Journal:	*ChemComm*
Manuscript ID	CC-COM-06-2019-004534.R1
Article Type:	Communication

COMMUNICATION

High yield synthesis and surface chemistry exchange of small gold hexagonal nanoprisms

Received 00th January 20xx,
Accepted 00th January 20xx

DOI: 10.1039/x0xx00000x

Katherinne I. Requejo, [a] Anton V. Liopo [ab] and Eugene R. Zubarev [a]*

A new seed-mediated synthesis of AuHNPs in high yield is described using hydroquinone as a weak reductant and poly(vinylpyrrolidone) as a shape-directing additive. We obtain distinct and small edge lengths of AuHNPs with long-term shape stability. Also, PVP enhances the monodispersity and enables higher stability of functionalized nanoprisms.

Gold nanoprisms are two-dimensional anisotropic nanostructures that have received significant attention in recent years.[1,2] The sharp features of nanoprisms have enabled their use as substrates for surface enhanced Raman scattering (SERS) of various analytes due to the localization of high electromagnetic fields at the vertices.[3–5] Another study demonstrated that nanoprisms with tailored surface plasmon resonance (SPR) bands enhance the signal for optical coherence tomography and present high photothermal performance.[6] Current synthetic protocols such as photochemical, biological and wet chemical methods have produced a mixture of triangular, truncated triangular and hexagonal shapes with edge lengths from 100 nm up to several micrometers, but often with high polydispersity and yields around 60-70%.[7–9] Only few protocols have reported improvement in shape yield for large size nanoprisms or the preparation of nanoprisms with edge lengths below 100 nm with yields of 70-80%.[3,10,11] The synthesis of small size gold hexagonal nanoprisms (AuHNPs) was demonstrated for an edge length of 70 nm with shape yield of 80% by the seed-mediated protocol utilizing the surfactant cetyltrimethylammonium bromide (CTAB).[12] Thus, there is a need to develop reproducible methods for the synthesis of small AuHNPs in high yield to enable biomedical applications such as diagnostics and therapy. The interest in obtaining small size nanostructures not only relies on the different optical properties, but also on the rapid clearance from the body when compared to large size nanomaterials as shown for gold nanorods.[13] Because there is a dynamic exchange between surfactant molecules forming the bilayer around nanocrystals and free surfactant in solution, cytotoxicity has been a major issue. For biomedical applications, it is essential to replace the surfactant from the surface of the AuHNPs by biocompatible ligands such as thiol-terminated poly(ethylene glycol) PEG-SH.[14] Functionalization of other anisotropic shapes such as nanorods[15,16] and nanotriangles[17–19] has been widely reported, but few studies exist on the surface modification of AuHNPs.[5] Here, we present a novel seed-mediated protocol of AuHNPs with hydroquinone as a reductant. By modifying reagent concentrations of the growth solutions such as hydroquinone, seed particles and iodide ions, AuHNPs with smaller edge lengths when compared to previous studies were produced in high yield. It was found that nanomolar concentration of 10 kDa poly(vinylpyrrolidone) (10PVP) improved the monodispersity of nanoprisms and conferred higher colloidal stability of functionalized nanoprisms which may enable potential biomedical applications.

Hydroquinone has been used for the formation of silver nanoprisms and gold nanorods,[20,21] but it has not been reported so far for the synthesis of AuHNPs. In the present seed-mediated synthesis, the first growth solution (GS 1) is used for the overgrowth of the seed particles and the second growth solution (GS 2) is where nanoprisms growth occurs (See SI). Both growth solutions initially contain Au(III) ions, the stabilizing agent cetyltrimethylammonium chloride (CTAC), sodium iodide (NaI) and hydroquinone. This synthesis is referred to as control sample because the polymer additive is not present in GS 2. The as synthesized seed solution, which has a concentration of gold atoms of 167 μM, is always diluted with CTAC solution before transferring it to GS1. Initially, we aimed to replace only the weak reductant from the gold nanotriangles synthesis with ascorbic acid reported by Scarabelli *et al.*[22] while keeping other reagent concentrations the same. The effect of hydroquinone concentration was evaluated from 10 to 20 times (10x-20x, 6-12 mM) with respect to Au(III) ions concentration in GS 2. Fig. 1A shows that as the amount of hydroquinone increases, the SPR band blue shifts from 730 to 650 nm indicating a decrease of the edge length. Similar to the seeded synthesis of gold nanotriangles, the nanoprisms growth is completed within 2 h and longer reaction times do not produce any increase in absorbance nor changes in the SPR band position. Since hydroquinone

[a] *Department of Chemistry, Rice University, Houston, Texas 77005, USA. E-mail: zubarev@rice.edu*
[b] *Texas A&M Health Science Center, Houston, Texas 77030, USA.*
Electronic Supplementary Information (ESI) available: Experimental section, additional spectra and TEM images. See DOI: 10.1039/x0xx00000x

concentration was fixed at 10x (2 mM) in GS 1, its effect was also assessed. Fig. 1B presents the variation of the SPR band as weak reductant concentration changes from 10x to 20x in GS 2 for different amounts of hydroquinone in GS 1 (3x-10x). There was not a large difference in the SPR band values among distinct concentrations of hydroquinone in GS 1, but the amount of spherical impurities was reduced when 10x was used for the whole range of values in GS 2 (Fig. 1A).

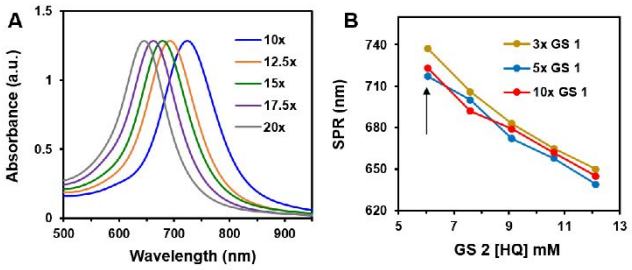

Fig. 1 (A) Normalized UV-Vis spectra of AuHNPs synthesized with different amounts of hydroquinone (HQ) in GS 2 for 10x = 2 mM HQ in GS 1 (red line in B) and 150 µL seeds. (B) Variation of SPR band of AuHNPs as a function of HQ concentration in GS 2 for three amounts of HQ in GS 1, 3x = 0.6 mM.

Overall, the nanoprisms obtained with 10x hydroquinone in GS 2 possess hexagonal and triangular shapes with a shape yield of 95% for nanoprisms and 80% for hexagons (Fig. S1). The edge length of the AuHNPs is below 100 nm which has been rarely synthesized by wet chemical method at room temperature.[12,23] Although the nanoprisms synthesized under these conditions were monodisperse, the TEM images still showed the presence of some nanotriangles as part of the large population of hexagons (Fig. S1). Next, we further confirmed the choices of hydroquinone concentrations in both growth solutions by synthesizing nanoprisms with 5 and 10 times diluted seeds. Fig. S2A,C shows the UV-Vis spectra for both seeds conditions with 20x hydroquinone in GS 1, which showed an improvement in nanoprisms quality as compared to 10x, and different amounts of weak reductant in GS 2. As we determined previously (Fig. 1), only 10x hydroquinone in GS 2 formed monodisperse nanoprisms in high yield with longer SPR band (Fig. S2B,D) when compared to the synthesis with higher concentrations of a weak reductant. Therefore, subsequent experiments were conducted with fixed amounts of hydroquinone of 20x (4.1 mM) and 10x (6.0 mM) for GS 1 and GS 2, respectively, with 10 times diluted seeds as the optimal reaction conditions.

Because size control can be achieved by modifying the amount of seeds added to the growth solutions,[24,25] we evaluated specific seed volumes added to GS 1 to produce monodisperse nanoprisms of sizes below 100 nm. Fig. S3A shows the UV-Vis spectra of nanoprisms obtained with 200-800 µL seeds and the SPR band blue shifts from 680 to 520 nm. When 200 µL seeds was used, it generated one of the largest size of nanoprisms in high yield (Fig. S3B), while 400 µL and higher volumes of seeds formed mostly circular plates and nanospheres, respectively (Fig. S3C-E). Thus, seeds volumes below 400 µL were assessed to determine distinct sizes of nanoprisms. The use of 50 µL seeds formed nanoprisms in low yield as shown in Fig. 2A. Increasing the volume of seeds to 100-150 µL produced a SPR band around 700 nm corresponding to the largest size of nanoprisms with the edge length of 82 nm (Fig. 2B). Values of seeds above 150 µL up to 300 µL blue shifted the SPR band progressively from 680 to 620 nm enabling the synthesis of small AuHNPs with tunable edge length from 68 to 50 nm (Fig. 2C,D). The histograms of edge length distribution for different sizes of AuHNPs synthesized with the optimal range of seeds amounts are shown in Fig. S4.

Once the size controlled synthesis of monodisperse small AuHNPs was identified, the next aim was to increase the shape yield of hexagons to above 90% with respect to nanotriangles. It has been reported that iodide ions preferentially adsorb on Au(111) facets and act as shape directing agents for nanoprisms growth.[26,27] Therefore, NaI concentration was varied in GS 2 which directly influences the nanoprisms growth. Fig. 3 shows the changes in the SPR band by modifying NaI from 37.5 to 137.5 µM for 150 µL seeds. Increasing the iodide concentration red shifted the SPR band to 700 nm and further increasing the concentration in GS 2 blue shifted the band. At low amounts of NaI, the incomplete adsorption on Au(111) facets led to nanoprisms in low yield and formed rod-like shapes (Fig. S5A), whereas very high amounts of iodide ions passivated all gold facets producing smaller nanoprisms with slightly rounded vertices (Fig. S5B,C). Similar results were obtained by changing iodide concentration for seeds volumes of 200-300 µL. However, the optimal iodide ion concentration was different for each seed amount to obtain monodisperse nanoprisms with hexagonal shape yield of 85-88%.

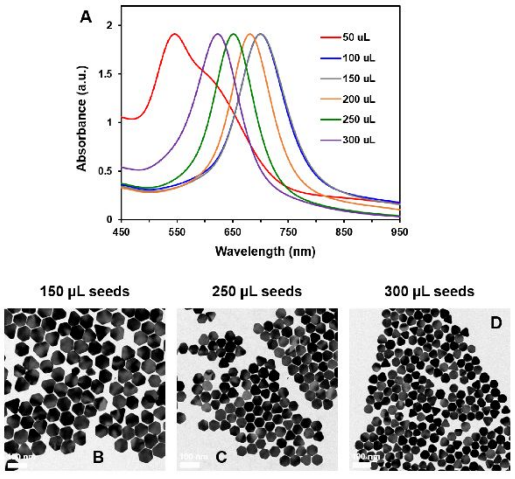

Fig. 2 (A) Normalized UV-Vis spectra of AuHNPs synthesized with different volumes of seeds (50-300 µL) added to GS 1 for 20x HQ in GS 1 and 10x HQ in GS 2. TEM images of AuHNPs for (B) 150 µL, (C) 250 µL and (D) 300 µL seeds. Scale bars are 100 nm.

Several investigations and mechanistic studies have determined the key factors for the kinetically-controlled formation of nanoprisms.[28] There is a general agreement that the final morphology of a nanostructure is dictated by the interplay between the seed structure and size and the synthetic conditions such as the use of facet selective ligands[29] or the type of weak reductant. Single-twinned seeds lead to the formation of triangular nanoprisms whereas twinned seeds with parallel planes produce hexagonal nanoprisms.[30]

Although there is no report on the preparation of high yield of twinned seeds with parallel planes, recent studies have reported the synthesis of single-twinned and multiple-twinned seeds by oxidative etching of anisotropic nanostructures.[31,32]

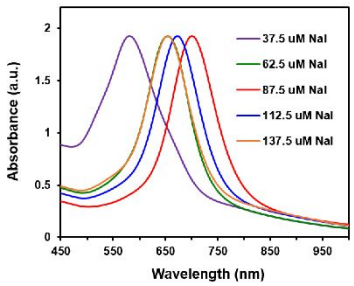

Fig. 3 Normalized UV-Vis spectra of AuHNPs synthesized with different amounts of NaI (37.5-137.5 μM) added to GS 2 for 150 μL seeds.

By changing the amount of hydroquinone, seeds and iodide ions in the growth solutions, we have been able to tune the size of AuHNPs below 100 nm, but other parameters need to be assessed to further improve the shape yield of hexagons. Polyvinylpyrrolidone (PVP) has been widely used at high concentration as capping agent, weak reductant and shape directing agent for the synthesis of gold nanoprisms or nanoplates of very large dimensions with edge lengths from 80 nm to 1 μm.[33–35] Our previous investigations on gold nanorods syntheses suggest that PVP stabilizes the surface of the nanocrystal and modifies the dimensions.[36,37] Because higher shape yield of small gold nanorods was achieved, we decided to assess the effect of PVP concentration and its molecular weight on the dimensions and shape yield of AuHNPs.

Fig. S6A presents the UV-Vis spectra of nanoprisms obtained with different concentrations of 10PVP added at 15 min of reaction for the synthesis with 150 μL seeds. The narrow range of nanomolar concentration of PVP (0.1-0.5 μg/mL) produced broadening and a blue shift of the SPR band as the amount of polymer was increased. Thus, the monodispersity and shape yield of AuHNPs were reduced despite of the smaller edge lengths. When different molecular weights from 5 to 360 kDa PVP were utilized and the concentration was decreased to 0.05 μg/mL, monodisperse AuHNPs of specific sizes were obtained depending on the molecular weight of the polymer (Fig. S6B). The use of 5PVP did not change the SPR band position when compared to the control, but as the molecular weight was increased to 10 and 55 kDa, the SPR band blue shifted. Although AuHNPs in high yield (89%) were obtained by incorporating PVP during the growth, the shape yield was similar to that of the control (87%). Further increasing the molecular weight to 360PVP produced the same SPR band as 55PVP, but the polydispersity was greatly increased as indicated by the band broadening. Subsequent experiments considered only 10PVP (0.05 μg/mL) added at 15 min after the start of the reaction for different volumes of seeds ranging from 150 to 300 μL. For the synthesis with 150 μL seeds, the blue shift of the SPR band indicated a decrease in the edge length of AuHNPs (Fig. 4A). Moreover, AuHNPs synthesized in the presence of small amounts of 10PVP showed a reduction in the full width at half maximum of 31 nm when compared to the control indicating an increase in monodispersity of AuHNPs (Fig. 4A). In contrast, the SPR band position did not change for the experiments with 200-300 μL seeds. Only for the AuHNPs synthesis with 150 μL seeds and polymer, a decrease in edge length of 8 nm was obtained (Fig. 4B-E). This reduction in edge length suggests that PVP adsorbs to the lateral sides of the growing nanoprisms in addition to the top and bottom surfaces which are Au(111) facets.[34] Since the polymer was added at 15 min of the reaction, PVP was able to stabilize the growing nanoprisms at an earlier stage for the large size AuHNPs whose growth takes longer when compared to small nanoprisms. We chose 15 min of the reaction because the PVP addition at earlier reaction times did not form AuHNPs in high yield. Regarding the standard deviation of edge length, it is lower for the sample with 10PVP which confirms the enhanced monodispersity of AuHNPs.

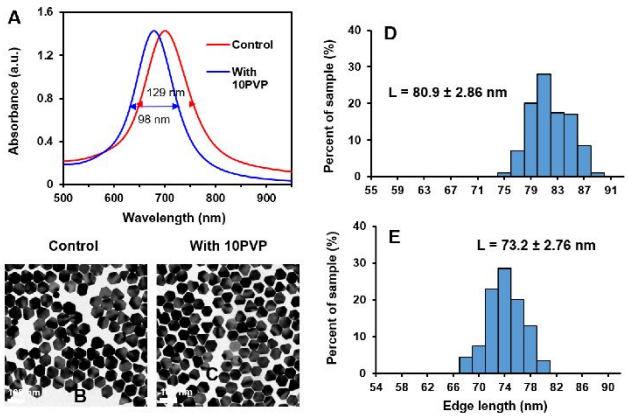

Fig. 4 (A) Normalized UV-Vis spectra of AuHNPs synthesized without (control) and with 0.05 μg/mL 10 kDa PVP (10PVP) added at 15 min of growth (GS 2) for 150 μL seeds. TEM images and histograms of edge length (L) distribution of AuHNPs control (B,D) and sample with polymer (C,E). Scale bars are 100 nm.

Furthermore, the thickness of vertically aligned AuHNPs was measured from TEM images and similar average thickness of 13-15 nm was determined for the control and samples with PVP (Tables S1, S2). Since the thickness of AuHNPs diminished for the experiments with 150 μL and 200 μL seeds in the presence of 10PVP, the polymer is inhibiting the deposition of gold atoms on the planar Au(111) facets at the early stages of growth. Therefore, the aspect ratio (edge length/thickness) of AuHNPs can be tuned from 3.7 to 5.6. The volume of AuHNPs was reduced in 0.22-0.25% only for the syntheses with 150 μL and 200 μL seeds and 10PVP as compared to the control (Tables S1, S2). The fast reaction growth (when 250 μL or 300 μL seeds is used) produces smaller nanoprisms within 15 min and the polymer cannot alter their dimensions. In the case of the nanotriangles that comprised around 10% of the nanoprisms, the edge length was 5 nm smaller than that of hexagons for each specific size. This indicates a possible shape transition from triangle to hexagon during growth due to the formation of parallel twin planes at early stages.[38] Although our seed-mediated protocol produces nanoprisms with hexagonal and triangular shapes as reported by others,[33,39,40] the significance of our work is the formation of nanoprisms

with smaller edge lengths and higher shape yield of hexagons (85-89%) by adjusting reagent concentrations and using PVP additive during the growth.

AuHNPs functionalization was conducted with 11-mercaptoundecyltrimethylammonium bromide (MUTAB) which is a thiolated compound with the headgroup of CTAB. Stabilization of AuHNPs in solution is due to the formation of gold-sulfur covalent bonds and MUTAB is expected to form a monolayer around the nanoprisms.[15] Zeta potential measurements of CTAC and MUTAB coated AuHNPs were similar and positive (Table S1), but a higher zeta potential value was observed for MUTAB protected nanoprisms synthesized with 10PVP suggesting that small amounts of polymer increase the stability of AuHNPs. It has been reported that the use of 10PVP to coat small metallic nanoparticles enhances the stability during silica shell growth.[41] Therefore, a possible explanation of why the zeta potential is more positive might be because PVP (neutral and amphiphilic polymer) favors the higher packing density of MUTAB on the nanoprisms surface which has great promise for incorporation into mammalian cells with negative charge.[16]

Since very few investigations have reported on the shape stability of AuHNPs,[23] we analyzed nanoprisms prepared with 10PVP after 6 months by UV-Vis spectroscopy and TEM. Fig. S7 shows identical UV-Vis spectra after synthesis and after 6 months for AuHNPs obtained with 200 µL seeds and the TEM images confirm that AuHNPs retain their shape. Besides, the possibility of shape transformation from triangles to hexagons over time was unlikely because the shape yield after 6 months was similar to AuHNPs after the synthesis. Thus, our reproducible hydroquinone assisted seed-mediated protocol presents the benefit of long-term shape stability when AuHNPs are stored in low CTAC concentration at room temperature.

We presented a novel hydroquinone-assisted seeded protocol for the synthesis of small AuHNPs in high yield with edge lengths from 50 to 81 nm and long-term shape stability. Hydroquinone favors the kinetically-controlled production of nanoprisms which improves their yield and quality.[20] By synthesizing AuHNPs with 10PVP, AuHNPs monodispersity is improved and the colloidal stability is enhanced after surface modification with MUTAB. Since higher shape yield (above 90%) of small hexagons is still envisioned for possible biomedical applications, future studies should investigate the effect of distinct polymers on the seed particles preparation to obtain a higher population of twinned seeds with 2D morphology.

Acknowledgement: This work was supported by NSF grant DMR-1105878.

Notes and references

1 J. E. Millstone, S. J. Hurst, G. S. Métraux, J. I. Cutler and C. A. Mirkin, *Small*, 2009, **5**, 646-664.
2 S. E. Lohse, N. D. Burrows, L. Scarabelli, L. M. Liz-Marzán and C. J. Murphy, *Chem. Mater.*, 2014, **26**, 34-43.
3 G. Lin, W. Lu, W. Cui and L. Jiang, *Cryst. Growth Des.*, 2010, **10**, 1118-1123.
4 I. Pastoriza-Santos, R. A. Alvarez-Puebla and L. M. Liz-Marzán, *Eur. J. Inorg. Chem.*, 2010, 4288-4297.
5 H. Yin, Y. Guo, X. Cui, W. Lu, Z. Yang, B. Yang and J. Wang, *Nanoscale*, 2018, **10**, 15058-15070.
6 X. Jiang, R. Liu, P. Tang, W. Li, H. Zhong, Z. Zhou and J. Zhou, *RSC Adv.*, 2015, **5**, 80709-80718.
7 X. Sun, S. Dong and E. Wang, *Langmuir*, 2005, **21**, 4710-4712.
8 H. -C. Chu, C. -H. Kuo and M. H. Huang, *Inorg. Chem.*, 2006, **45**, 808-813.
9 S. Balasubramanian, S. R. Bezawada and D. Raghavachari, *ACS Sustainable Chem. Eng.*, 2016, **4**, 3830-3839.
10 Y. Zhai, J. S. DuChene, Y. -C. Wang, J. Qiu, A. C. Johnston-Peck, B. You, W. Guo, B. DiCiaccio, K. Qian, E. W. Zhao, F. Ooi, D. Hu, D. Su, E. A. Stach, Z. Zhu and W. D. Wei, *Nat. Mater.,* 2016*, **15**, 889-896.*
11 S. He, J. Hai, T. Li, S. Liu, F. Chen and B. Wang, *Nanoscale*, 2018, **10**, 18805-18811.
12 T. K. Sau and C. J. Murphy, *J. Am. Chem. Soc.*, 2004, **126**, 8648-8649.
13 Z. Li, S. Tang, B. Wang, Y. Li, H. Huang, H. Wang, P. Li, C. Li, P. K. Chu and X. -F. Yu, *ACS Biomater. Sci. Eng.*, 2016, **2**, 789-797.
14 V. W. K. Ng, R. Berti, F. Lesage and A. Kakkar, *J. Mater. Chem. B*, 2013, **1**, 9-25.
15 L. Vigderman, P. Manna and E. R. Zubarev, *Angew. Chem. Int. Ed.*, 2012, **51**, 636-641.
16 A. V. Liopo, E. R. Zubarev and A. A. Oraevsky, in *Nanotheranostics*, ed. B. Singh, M. S. Sachdeva, A. V. Liopo, Studium Press, Houston, 2015, 7, 189-230.
17 K. Nambara, K. Niikura, H. Mitomo, T. Ninomiya, C. Takeuchi, J. Wei, Y. Matsuo and K. Ijiro, *Langmuir*, 2016, **32**, 12559-12567.
18 X. Xie, J. Liao, X. Shao, Q. Li and Y. Lin, *Sci. Rep.,* 2017*, **7**, 1-9.*
29 S. R. Bhattarai, P. J. Derry, K. Aziz, P. K. Singh, A. M. Khoo, A. S. Chadha, A. Liopo, E. R. Zubarev and S. Krishnan, *Nanoscale*, 2017, **9**, 5085-5093.
20 S. T. Gentry and S. D. Levit, *J. Phys. Chem. C*, 2009, **113**, 12007-12015.
21 L. Vigderman and E. R. Zubarev, *Chem. Mater.*, 2013, **25**, 1450-1457.
22 L. Scarabelli, M. Coronado-Puchau, J. J. Giner-Casares, J. Langer and L. M. Liz-Marzán, *ACS Nano*, 2014, **8**, 5833-5842.
23 P. Kaur and B. Chudasama, *RSC Adv.*, 2014, **4**, 36006-36011.
24 B. -H. Kim, J. -H. Oh, S. H. Han, Y. -J. Yun and J. -S. Lee, *Chem. Mater.*, 2012, **24**, 4424-4433.
25 C. -W. Chou, H. -H. Hsieh, Y. -C. Hseu, K. -S. Chen, G. -J. Wang, H. -C. Chang, Y. -L. Pan, Y. -S. Wei, K. H. Changa and Y. -W. Harn, *Phys. Chem. Chem. Phys.*, 2013, **15**, 11275-11286.
26 J. E. Millstone, W. Wei, M. R. Jones, H. Yoo and C. A. Mirkin, *Nano Lett.*, 2008, **8**, 2526-2529.
27 J. S. DuChene, W. Niu, J. M. Abendroth, Q. Sun, W. Zhao, F. Huo and W. D. Wei, *Chem. Mater.*, 2013, **25**, 1392-1399.
28 Y. Xia, Y. Xiong, S. E. Skrabalak, *Angew. Chem. Int. Ed.*, 2009, **48**, 60-103.
29 G. Zhan, L. Ke, Q. Li, J. Huang, D. Hua, A. -R. Ibrahim and D. Sun, *Ind. Eng. Chem. Res.*, 2012, **51**, 15753-15762.
30 C. Lofton and W. Sigmund, *Adv. Funct. Mater.*, 2005, **15**, 1197-1208.
31 G. González-Rubio, T. Milagres de Oliveira, T. Altantzis, A. La Porta, A. Guerrero-Martínez, S. Bals, L. Sacarabelli and L. M. Liz-Marzán, *Chem. Commun.*, 2017, **53**, 11360-11363.
32 A. Sánchez-Iglesias, N. Winckelmans, T. Altantzis, S. Bals, M. Grzelczak and L. M. Liz-Marzán, *J. Am. Chem. Soc.*, 2017, **139**, 107-110.
33 C. S. Ah, Y. J. Yun, H. J. Park, W. -J. Kim, D. H. Ha and W. S. Yun, *Chem. Mater.*, 2005, **17**, 5558-5561.
34 A. A. Umar, M. Oyama, M. M. Salleh and B. Y. Majlis, *Cryst. Growth Des.*, 2009, **9**, 2835-2840.
35 A. A. Umar, M. Oyama, M. M. Salleh and B. Y. Majlis, *Cryst. Growth Des.*, 2010, **10**, 3694-3698.
36 K. I. Requejo, A. V. Liopo, P. J. Derry and E. R. Zubarev, *Langmuir*, 2017, **33**, 12681-12688.
37 K. I. Requejo, A. V. Liopo and E. R. Zubarev, *ChemistrySelect*, 2018, **3**, 12192-12197.
38 D. Alloyeau, W. Dachraoui, H. Belkahla, G. Wang, S. Ammar, O. Ersen, A. Wisnet, F. Gazeau and C. Ricolleau, *Nano Lett.*, 2015, **15**, 2574-2581.
39 S. Hong, J. A. I. Acapulco Jr., H. -J. Jang, A. S. Kulkarni and S. Park, *Bull. Korean Chem. Soc.*, 2014, **35**, 1737-1742.
40 G. Wang, S. Tao, Y. Liu, L. Guo, G. Qian, K. Ijiro, M. Maeda and Y. Yin, *Chem. Commun.*, 2016, **52**, 398-401.
41 C. Graf, D. L. J. Vossen, A. Imhof and A. van Blaaderen, *Langmuir*, 2003, **19**, 6693-6700.

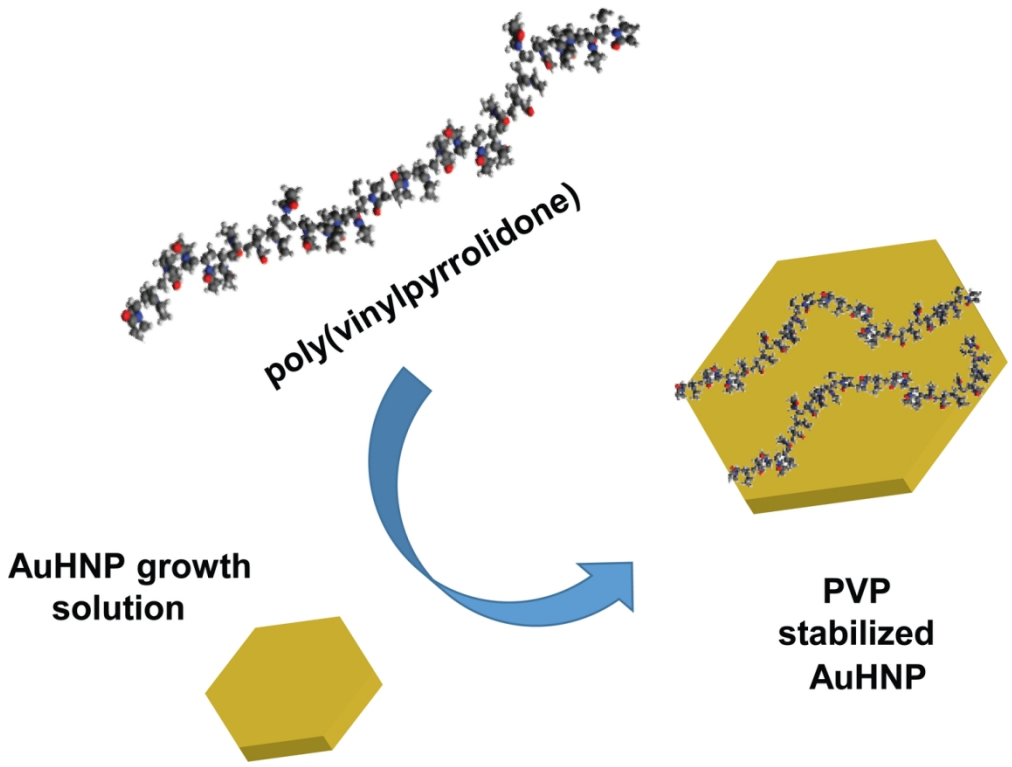

128x105mm (300 x 300 DPI)